Available online at www.sciencedirect.com

ScienceDirect

Procedia Structural Integrity 2 (2016) 3475–3482

Structural Integrity Procedia

www.elsevier.com/locate/procedia

21st European Conference on Fracture, ECF21, 20-24 June 2016, Catania, Italy

Modelling and fatigue assessment of steel rollers with failure occurring at the weld root based on the local strain energy

F. Berto[a,b], A. Campagnolo[c], F. Chebat[d], M.Cincera[d], T. Welo[b]

[a]*Department of Management and Engineering, Stradella San Nicola 3, 36100 Vicenza, Italy*
[b]*NTNU, Department of Engineering Design and Materials, Richard Birkelands vei 2b, 7491, Trondheim, Norway*
[c]*Department of Industrial Engineering, Via Venezia 1, 35131 Padova, Italy*
[d]*Rulli Rulmeca S.P.A.*

Abstract

Weldments geometry with failures occurring at the weld toe or at the weld root cannot, by its nature, be precisely defined. Parameters such as bead shape and toe or root radius vary from joint to joint even in well-controlled manufacturing operations. The worst case configuration can be achieved by modelling as a sharp, zero radius, notch both the toe and the weld root. The intensity of asymptotic stress distributions obeying Williams' solution are quantified by means of the Notch Stress Intensity Factors (NSIFs). For steel welded joints with failures originated from the weld roots, where the lack of penetration zone is treated as a crack-like notch, units for NSIFs are the same as conventional SIF used in LEFM. The different dimensionality of NSIFs for different notch opening angles does not allow a direct comparison of failures occurring at the weld toe or at the weld root. In order to overcome the problem related to the variability of the V-notch opening angle, a simple scalar quantity, i.e. the value of the strain energy density averaged in the structural volume surrounding the notch tip, has been introduced. This energy is given in closed form on the basis of the relevant NSIFs for modes I, II and III. The radius R_C of the averaging zone is carefully identified with reference to conventional arc welding processes being equal to 0.28 mm for welded joints made of steel.
The local-energy based criterion is applied here to steel welded rollers produced by Rulmeca subjected to prevailing mode I (with failures at the weld root). The aim of the paper is firstly to describe the employed methodology for the fatigue assessment and secondly to show the first synthesis of fatigue data by means of local SED for a specific geometry.

Peer-review under responsibility of the Scientific Committee of ECF21.

Keywords: Welded Joints; Fatigue Strength; Notch Stress Intensity factor; Strain Energy Density, Elasticity.

* Corresponding author
E-mail address: berto@gest.unipd.it

Copyright © 2016 The Authors. Published by Elsevier B.V. This is an open access article under the CC BY-NC-ND license (http://creativecommons.org/licenses/by-nc-nd/4.0/).
Peer review under responsibility of the Scientific Committee of ECF21.
10.1016/j.prostr.2016.06.433

1. Introduction

Weld bead geometry cannot be precisely defined mainly because parameters such as bead shape, toe or root radius and length of lack of penetration vary from joint to joint even in well-controlled manufacturing operations (Radaj 1990, Taylor et al. 2002). It is, in fact well known that, the weld toe radius decreases with the local heat concentration of the welding process, i.e. it is extremely small for automated high-power processes, especially for laser beam welding. Since also conventional arc welding techniques result in small values of toe radius (Yakubovskii and Valteris 1989), in the Notch Stress Intensity Factor (NSIF) approach the weld toe region is modelled as a sharp notch and local stresses are given on the basis of the relevant mode I and mode II NSIFs (Yakubovskii and Valteris 1989, Dunn et al. 1997). When the opening angle at the weld toe is large enough to result in a non-singular contribution for stress components due to the mode II, the fatigue behaviour can be correlated only to mode I NSIF (Dunn et al. 1997). A comparison among different steel welded joints can be performed on the basis of the relevant theoretical stress concentration factors, after having imposed a fictitious notch radius ρ_f=1.0 mm. This value is valid only if the real radius at the weld toes and roots is thought of as zero (Lazzarin and Tovo 1998). Fatigue failure is generally characterized by the nucleation and growth of cracks. As widely discussed in the previous literature, the differentiation of two stages is “qualitatively distinguishable but quantitatively ambiguous” (Jiang and Feng 2004). In this context NSIFs were found capable of predicting not only the part of life spent in crack nucleation but also the total fatigue life (Berto and Lazzarin 2014, Ferro 2014, Radaj 2014, Radaj 2015).

This happens when a large amount of life is consumed at short crack depth, within the zone governed by the notch singularity at the weld toe or root. Different set of experimental data proved this behaviour. Dealing with transverse non-load-carrying fillet welded joints Lassen (1990) demonstrated that for various welding procedures, up to 40 percent of fatigue life was spent to nucleate a crack having a length of just 0.1 mm. Singh et al. (2003a, 2003b) showed by testing load-carrying fillet joints in AISI 304L that the number of cycles required for the crack to grow by 0.5 mm in excess of the original lack of penetration reached 70 percent of the total life.

From a theoretical point of view the NSIF-based approach cannot be applied to joints characterized by weld flank angles very different from 135 degrees or for comparing failures at the weld root (2α=0°) or weld toe (2α=135°). That is simply because units for mode I NSIF are MPa(m)$^{\beta}$, where the exponent β depends on the V-notch angle, according to the expression $\beta = 1- \lambda_1$, λ_1 being Williams’ eigenvalue (Williams 1952). This problem has been overcome in some recent papers by using the mean value of the strain energy density range (SER) present in a control volume of radius R_C surrounding the weld toe or the weld root. SER was given in closed form as a function of the relevant NSIFs, whereas R_C was thought of as dependent on welded material properties. The approach, reminiscent of Neuber “elementary volume” concept, was later applied to welded joints under multiaxial load conditions (Lazzarin et al. 2004). The simple volume is not so different from that already drawn by Sheppard (1991) while proposing a volume criterion based on local stresses to predict fatigue limits of notched components. Some analogies exist also with the highly stressed volume (the region where 90% of the maximum notch stress is exceeded) proposed by Sonsino dealing with high cycle strength of welded joints (Sonsino 1995).

The same based on energy approach has been employed here for the fatigue assessment of steel rollers made by Rulmeca with failure occurring at the weld root. The rollers considered in the present investigation belong to the category PSV which is particularly suited to conveyors that operate in very difficult conditions, where working loads are high, and large lump size material is conveyed; and yet, despite these characteristics, they require minimal maintenance. The bearing housings of the PSV series are welded to the tube body using autocentralising automatic welding machines utilizing a continuous wire feed.

From the point of view of the fatigue behavior under load, the weakest point of the entire structure is the lack of penetration of the weld root. Therefore, if the roller is loaded well above its declared nominal admitted load (Rulmeca Bulk Catalogue 2014) it would experience fatigue failure starting at the level of the weld root.

The aims of the present work are:

- to describe the procedure for modelling the roller by using the finite element method combined with three-dimensional analyses (the procedure is described in more detail in (Berto et al. 2016));
- to describe the sensitivity of the model to the length of the lack of penetration;
- to show the procedure for evaluating the SED in a control volume surrounding the crack tip in a real component describing the trend of the SED in a three-dimensional model;

- to verify if a scatter band ΔW-N (strain energy range – number of cycles to failure) summarising about 1200 fatigue data from welded joints with the majority of failures originated from the weld toes can be applied also to welded joints with failures from the weld roots and in particular to the considered rollers;
- with reference to the just mentioned point some preliminary fatigue tests from two different geometries belonging to the family of rollers called PSV4 and characterized by a different length, have been carried out and summarised here by means of local SED.

An extended version of the present manuscript can be found in (Berto et al. 2016).

2. Approach based on the local SED: analytical preliminaries

The degree of singularity of the stress fields due to re-entrant corners was established by Williams both for mode I and mode II loading (Williams 1952). When the weld toe radius ρ is set to zero, NSIFs quantify the intensity of the asymptotic stress distributions in the close neighbourhood of the notch tip. By using a polar coordinate system (r, θ) having its origin located at the sharp notch tip, the NSIFs related to mode I and mode II stress distribution are (Gross and Mendelson 1972):

$$K_1^N = \sqrt{2\pi} \lim_{r\to 0^+} r^{1-\lambda_1} \sigma_{\theta\theta}(r, \theta = 0) \tag{1}$$

$$K_2^N = \sqrt{2\pi} \lim_{r\to 0^+} r^{1-\lambda_2} \tau_{r\theta}(r, \theta = 0) \tag{2}$$

where the stress components $\sigma_{\theta\theta}$ and $\tau_{r\theta}$ have to be evaluated along the notch bisector (θ=0).

Dealing with mode III loading an extension of the definition proposed by Gross and Mendelson (1972) has been carried out in (Qian and Hasebe 1997, Zappalorto et al. 2008):

$$K_3^N = \sqrt{2\pi} \lim_{r\to 0^+} r^{1-\lambda_3} \tau_{\theta z}(r, \theta = 0) \tag{3}$$

By means of Eqs. (1,2), it is possible to present Williams' formulae for stress components as explicit functions of the NSIFs. Then, mode I stress distribution is (Lazzarin and Tovo 1996):

$$\begin{Bmatrix} \sigma_{\theta\theta} \\ \sigma_{rr} \\ \tau_{r\theta} \end{Bmatrix}_{\rho=0} = \frac{1}{\sqrt{2\pi}} \frac{r^{\lambda_1-1} K_1^N}{(1+\lambda_1)+\chi_1(1-\lambda_1)} \left[\begin{Bmatrix} (1+\lambda_1)\cos(1-\lambda_1)\theta \\ (3-\lambda_1)\cos(1-\lambda_1)\theta \\ (1-\lambda_1)\sin(1-\lambda_1)\theta \end{Bmatrix} + \chi_1(1-\lambda_1) \begin{Bmatrix} \cos(1+\lambda_1)\theta \\ -\cos(1+\lambda_1)\theta \\ \sin(1+\lambda_1)\theta \end{Bmatrix} \right] \tag{4}$$

Mode II stress distribution is:

$$\begin{Bmatrix} \sigma_{\theta\theta} \\ \sigma_{rr} \\ \tau_{r\theta} \end{Bmatrix}_{\rho=0} = \frac{1}{\sqrt{2\pi}} \frac{r^{\lambda_2-1} K_2^N}{(1-\lambda_2)+\chi_2(1+\lambda_2)} \left[\begin{Bmatrix} -(1+\lambda_2)\sin(1-\lambda_2)\theta \\ -(3-\lambda_2)\sin(1-\lambda_2)\theta \\ (1-\lambda_2)\cos(1-\lambda_2)\theta \end{Bmatrix} + \chi_2(1+\lambda_2) \begin{Bmatrix} -\sin(1+\lambda_2)\theta \\ \sin(1+\lambda_2)\theta \\ \cos(1+\lambda_2)\theta \end{Bmatrix} \right] \tag{5}$$

Mode III stress distribution is:

$$\begin{aligned} \tau_{zr} &= \frac{K_3^N}{\sqrt{2\pi}} r^{\lambda_3-1} \sin(\lambda_3\theta) \\ \tau_{z\theta} &= \frac{K_3^N}{\sqrt{2\pi}} r^{\lambda_3-1} \cos(\lambda_3\theta) \end{aligned} \tag{6}$$

All stress and strain components in the highly stressed region are correlated to mode I, mode II and mode III NSIFs. Under plane strain hypothesis, the strain energy included in a semicircular sector is (Lazzarin and Zambardi 2001, Berto et al. 2015):

$$\Delta\overline{W} = \frac{e_1}{E}\left[\frac{\Delta K_1^N}{R_C^{1-\lambda_1}}\right]^2 + \frac{e_2}{E}\left[\frac{\Delta K_2^N}{R_C^{1-\lambda_2}}\right]^2 + \frac{e_3}{E}\left[\frac{\Delta K_3^N}{R_C^{1-\lambda_3}}\right]^2 \tag{7}$$

where R_C is the radius of the semicircular sector and e_1, e_2 are functions that depend on the opening angle 2α and on the Poisson's ratio ν, while e_3 depends only on the notch opening angle. A rapid calculation, with $\nu = 0.3$, can be made for e_1 and e_2 by using the following expressions (Lazzarin and Zambardi 2001):

$$e_1 = -5.373\cdot10^{-6}(2\alpha)^2 + 6.151\cdot10^{-4}(2\alpha) + 0.1330 \tag{8}$$

$$e_2 = 4.809\cdot10^{-6}(2\alpha)^2 - 2.346\cdot10^{-3}(2\alpha) + 0.3400 \tag{9}$$

where 2α is in degrees. Dealing with failures originated at the crack tip (i.e. weld root) Eq. (7) can be simplified as follows:

$$\Delta\overline{W} = \frac{1}{ER_C}\left[e_1\Delta K_1^2 + e_2\Delta K_2^2 + e_3\Delta K_3^2\right] \tag{10}$$

The material parameter R_C can be estimated by using the fatigue strength $\Delta\sigma_A$ of the butt ground welded joints (in order to quantify the influence of the welding process, in the absence of any stress concentration effect) and the NSIF-based fatigue strength of welded joints having a V-notch angle at the weld toe constant and large enough to ensure the non singularity of mode II stress distributions. A convenient expression is (Lazzarin and Zambardi 2001):

$$R_C = \left(\frac{\sqrt{2e_1}\,\Delta K_{1A}^N}{\Delta\sigma_A}\right)^{\frac{1}{1-\lambda_1}} \tag{11}$$

where both λ_1 and e_1 depend on the V-notch angle. Eq. (11) will be applied in the next sections of the paper taking into account the experimental value ΔK_{1A}^N at 5 million cycles related to transverse non-load carrying fillet welded joints with $2\alpha = 135$ degrees at the weld toe. The hypothesis of constancy of R_C under mixed mode loads had been validated by Lazzarin and Zambardi (2001) by using experimental data mainly provided by Seweryn et al. (1997) and Kihara and Yoshii (1991). From a theoretical point of view the material properties in the vicinity of the weld toes and the weld roots depend on a number of parameters as residual stresses and distortions, heterogeneous metallurgical micro-structures, weld thermal cycles, heat source characteristics, load histories and so on. To device a model capable of predicting R_C and the fatigue life of welded components on the basis of all these parameters is really a task too complex. Thus, the spirit of this approach is to give a simplified method able to summarise the fatigue life of components only on the basis of geometrical information, treating all other effects only in statistical terms, with reference to a well-defined group of welded materials and, for the time being, to arc welding processes. Eq. (11) makes it possible to estimate the R_C value as soon as ΔK_{1A}^N and $\Delta\sigma_A$ are known. At $N_A = 5\cdot10^6$ cycles and in the presence of a nominal load ratio R equal to zero, a mean value ΔK_{1A}^N equal to 211 MPa mm$^{0.326}$ can be assumed (Livieri and Lazzarin, 2005). For butt ground welds made of ferritic steels Atzori and Dattoma (1983) found a mean value $\Delta\sigma_A = 155$ MPa (at $N_A = 5\cdot10^6$ cycles, with R=0). That value is in very good agreement with $\Delta\sigma_A = 153$ MPa recently obtained by Taylor at al. (2002) by testing butt ground welds fabricated of a low carbon steel. Then, by introducing the above mentioned value into Eq. (11), one obtains for steel welded joints with failures from the weld toe $R_C = 0.28$ mm. The choice of 5 million cycles as a reference value is due mainly to the fact that, according to Eurocode 3, nominal stress ranges corresponding to 5 million cycles can be considered as fatigue limits under constant amplitude load histories. It is worth noting that the simplified hypothesis of a semicircular core of radius R_C led to the assessment of a fatigue scatter band that exactly agreed with that of Haibach's normalised S-N band (Haibach 1989). In the case $2\alpha=0$ and fatigue crack initiation at the weld root Eq. (11) gives $R_C=0.36$ mm, by neglecting the mode II contribution and using $e_1=0.133$, Eq. (8), $\Delta K_{1A}^N = 180$ MPa mm$^{0.5}$ and, once again, $\Delta\sigma_A = 155$ MPa. There is a small difference with respect to the value previously determined, $R_C=0.28$ mm. However, in the safe direction, the proposal is to use $R_C=0.28$ mm also for the welded joints with failures from the weld roots which

is the case considered in the present manuscript. As opposed to the direct evaluation of the NSIFs, which needs very refined meshes, the mean value of the elastic SED on the control volume can be determined with high accuracy by using coarse meshes (Lazzarin et al. 2008, Lazzarin et al. 2010, Meneghetti et al. 2015).

3. Modelling of the rollers and evaluation of the local SED

The rollers considered in the present investigation belong to the series PSV which offer the highest quality and the maximum load capacity of Rulmeca's production (see Figure 1) (Rulmeca Bulk Catalogue 2014).

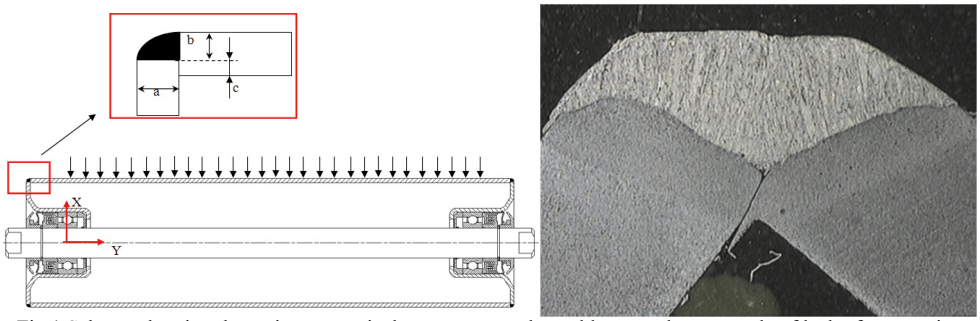

Fig.1 Scheme showing the main geometrical parameters at the weld root and an example of lack of penetration

Rollers PSV are particularly suited to conveyors that operate in very difficult conditions, where working loads are high, and large lump size material is conveyed; and yet, despite these characteristics, they require minimal maintenance. Typical types of application are: mines, caves, cement works, coal-fired electric utilities and dock installations. The effectiveness of the PSV roller sealing system provides the solution to the environmental challenges of dust, dirt, water, low and high temperatures.

Roller is made of the following main components:

- A mantel, constituted by a tube cut and machined using automatic numerically controlled machines, that guarantee and maintain the tolerances and the precision of the square cut.
- Two bearing housing made by a steel monolithic structure (in agreement with UNI EN 10111 characterized by a yield strength $170<\sigma_y<330$ MPa), deep drawn and sized to a forced fixed tolerance (ISO M7) at the bearing position. The thickness of the housings is proportional to the spindle diameter and to the bearing type, with thicknesses that are up to 5 mm, to guarantee the maximum strength for each application, including the heaviest.
- A spindle which sustains the roller when it is assembled into the troughing set supports. It is made from drawn steel, cut and machined by automatic numerically controlled machines. The spindle is ground to a precision tolerance, to guarantee a perfect match of bearings, seals. Spindle tolerance, together with bearing housing tolerances, functionally guarantees the autoalignment of the internal and outer bearing rings of the ball race resulting in a good performance even when the spindle deflection is extreme due to overloading.
- The seals components, which are meant to protect the bearing from harmful elements that may impinge from the outside or the inside of the roller, made of three main sections:
  1. external section: made of an external stone guard, a lip ring made from soft anti-abrasive rubber with a large contact surface onto a metal cover cap; that forms a self cleaning stage of seal in that it centrifugally repels water and dust naturally towards the outside;
  2. outward bearing protection: triple lip labyrinth in nylon PA6 greased to give further bearing protection;
  3. inward bearing protection, made of a sealing ring in nylon PA6 is positioned that provides an ample grease reservoir and also retains the grease near to the bearing even when there is a depression due to an abrupt change in temperature (pumping effect).
- Locking system: provided by means of the correctly located cir-clip, which is the most effective and the strongest system implemented in heavy rollers for belt conveyors.

The feature under investigation in this paper is the joint between tube and bearing housing.

The bearing housings of the PSV rollers are welded to the tube body using autocentralising automatic welding

machines utilising a continuous wire feed. Tube and bearing housing form a monolithic structure of exceptional strength which itself reduces to the minimum any imbalance in the roller. This guarantees the alignment and concentricity with respect to the external diameter of the component parts of the sealing system. The optimum balance and concentricity thus obtained allows these rollers to be used at the highest speeds, eliminating harmful vibration to the conveyor structure and the "hammer effect" on the bearings of the rollers.

From the point of view of the fatigue behavior under loading, the weakest point of the entire structure is the lack of penetration of the weld root. Therefore, if the roller is loaded well above its declared nominal admitted load (Rulmeca Bulk Catalogue 2014) it would experience fatigue failure starting at the level of the weld root. A detail of the weld root is shown in Figure 1, where the lack of penetration length is indicated as *c*.

The load on top of the roller is modelled typically as a uniformly distributed load on the longitudinal line of the roller.

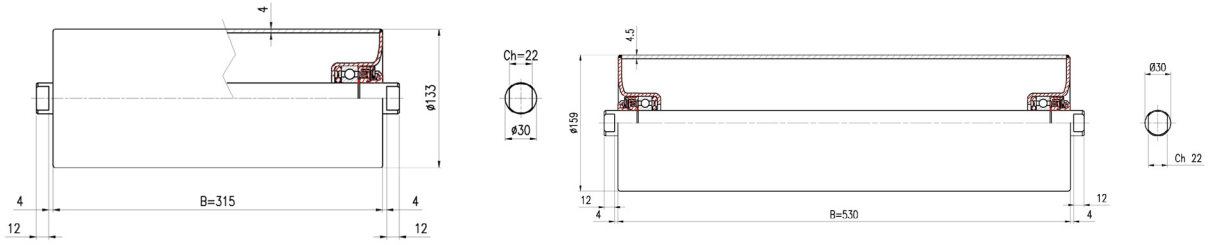

(a) (b)

Fig. 2.Geometry of the rollers: PSV4 133 315 (a) PSV4 159 530 (b)

Two geometries have been considered here and the details of the geometrical parameters are reported in Figure 2a and 2b for the two cases, named in the following as PSV4 133 315 and PSV4 159 530. For sake of brevity the modeling will be shortly described only for the first geometry. Further details are reported in (Berto et al. 2016).

The analysis of the stress fields in these welded details needed 3D models, because of their variability along the circular path described by the weld root. The two considered geometries reported in Figure 2 have been modelled by means of 20-node 3D finite elements implemented in the FE code ANSYS. Due to the symmetry of geometry and loading only one quarter of the geometry has been considered. The bearing has been considered of infinite stiffness and all the nodes of the bearing housing have been connected by means of rigid elements (links) to a master node. This special node has been placed on the symmetrical longitudinal axis of the roller in correspondence of the instantaneous rotation centre of the bearing. The rotation about the axis Z (ROT_Z) and the longitudinal displacement (U_Y, see Fig. 1) have been left unconstrained, while all other displacements and rotations of the master node have been constrained. The load has been distributed along the longitudinal line.

For each geometry two models were created: the first was mainly oriented to the determination of the point where the maximum principal stress and the maximum value of the strain energy density were located. Due to the complex geometry of the bearing housing in fact the point varies as a function of the geometry. In this case a regular fine mesh has been used with the aim also to determine the SIFs at the weld root.

The second model was characterized by a coarse mesh but by an accurate definition of the control volume where the strain energy density should be averaged. As just stated the mesh used in that case was coarse with a regular increasing spacing ratio in the direction of the position of the control volume mainly aimed to a correct positioning of the volume itself in the most critical region. All FE analyses have been carried out by means of 20-node finite elements under linear-elastic hypotheses.

4. Fatigue strength in terms of strain energy density averaged in a finite size volume

By using the first model with a regular and very fine mesh the SED has been evaluated circumferentially all around the roller in the zone surrounding the weld root. The maximum SED value occurs outside the line of the application of the load. The angle of rotation is strongly dependent on the geometry of the bearing housing. In the case of the roller PSV 133 315 the maximum SED occurs at about 30 degrees from the line of load application. In that point all the modes of failure are contemporary present as will be discussed in the following.

For this specific model an analysis of sensitivity of SED as a function of the length of the lack of penetration c

has been carried out (Berto et al. 2016). From a micrographic analysis conducted on a large amount of welded rollers c has been found to vary in the range between 0.6 and 1.0 mm. A typical image of the weld root is shown in Figure 1b. The sensitivity analysis has been made varying the length of the lack of penetration and evaluating the SED in a control volume of radius R_C=0.28 mm. The variation of the SED is very limited in the range of c considered. The SED varies from 0.31 MJ/m^3 to 0.35 MJ/m^3 for a value of *c* corresponding to 0.6 and 1.0 mm, respectively. Considering the low variation of the SED as a function of the initial lack of penetration, the length *c*=1 mm has been set in all FE analyses. This choice is in the safe direction because the worst configuration has been considered.

Some fatigue tests have been conducted on the two rollers shown in Figure 2 (Berto et al. 2016). A test system has been created for reproducing the service conditions on the roller. The load has been applied by means of an external counter-roll which press with a constant pressure the tested roller which rotates with a regular speed. Altogether 22 new tests have been carried out considering the two investigated geometries. The new results reconverted in terms of the local SED have been compared with the scatterband proposed for structural welded steels (Livieri and Lazzarin 2005). That band is shown in Figure 3 together with the new data. It is evident that the previous scatter band can be satisfactorily applied also to the new data from failure at the weld root of rollers tested at different load levels.

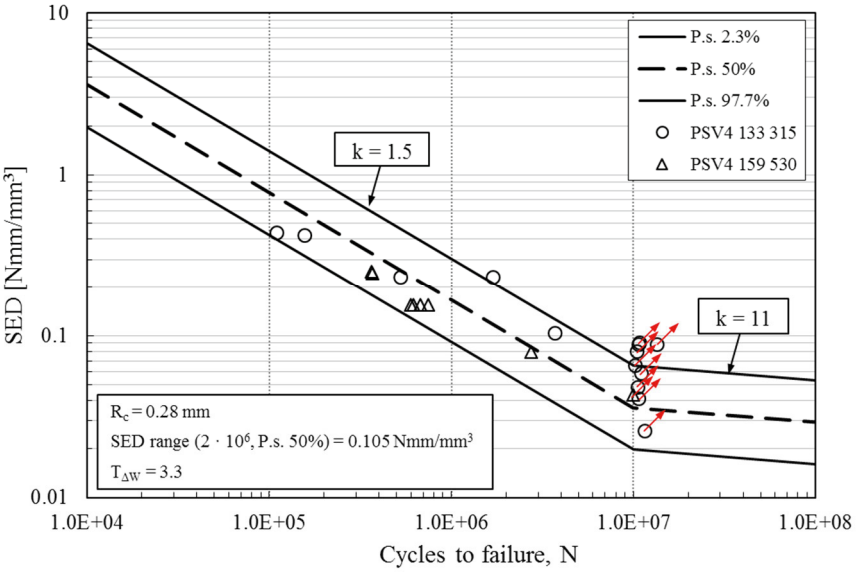

Fig. 3. Synthesis of new data in terms of local SED and comparison with the scatterband by Lazzarin and co-authors

Conclusions

The present paper deals with a local energy based approach employed for the fatigue assessment of rollers with failure occurring at the weld root. The rollers considered in the present investigation are particularly suited to conveyors that operate in very difficult conditions, where working loads are high, and large lump size material is conveyed; and yet, despite these characteristics, they require minimal maintenance. The bearing housings are welded to the tube body using autocentralising automatic welding machines utilizing a continuous wire feed.

From the point of view of the fatigue behavior under loading, the weakest point of the entire structure is the lack of penetration of the weld root. Therefore, if the roller is loaded well above its declared nominal admitted load (Rulmeca Bulk Catalogue 2014), it would experience fatigue failure starting at the level of the weld root. A detail of the weld root is shown in Figure 1b, where the lack of penetration length is indicated as *c*.

The rollers have been modelled by using the finite element method combined with three-dimensional analyses. The procedure for evaluating the local parameters in the zone close to the lack of penetration at the weld root has been described in the paper showing the low sensitivity of the model to the length of the lack of penetration. The detailed procedure for evaluating the SED in the control volume surrounding the crack tip in the weakest point of

the roller has been summarised (Berto et al. 2016). Some fatigue tests from two different geometries belonging to the family of rollers called PSV4 from Rulmeca production have been carried out and summarised here by means of local SED. It has been proved that the scatter band ΔW-N (strain energy range – number of cycles to failure), summarising about 1200 fatigue data from welded joints with the majority of failures originated from the weld toes, can be successfully applied also to welded joints with failures from the weld roots and in particular to the considered rollers geometry.

References

Atzori, B., Dattoma, V., 1983. A comparison of the fatigue behaviour of welded joints in steels and in aluminium alloys. IIW Doc XXXIII-1089-1983.

Berto, F., Lazzarin, P., 2014. Recent developments in brittle and quasi-brittle failure assessment of engineering materials by means of local approaches. Mater Sci Eng R Reports 75, 1–48.

Berto, F., Campagnolo, A., Lazzarin, P., 2015. Fatigue strength of severely notched specimens made of Ti–6Al–4V under multiaxial loading Fatigue Fract. Eng. Mater. Struct. 38, 503–517.

Berto, F., Campagnolo, A., Chebat, F., Cincera, M., Santini, M., 2016. Fatigue strength of steel rollers with failure occurring at the weld root based on the local strain energy values: modelling and fatigue assessment. Int. J. Fatigue 82, 643–657.

Dunn, M.L., Suwito, W., Cunningham, S., 1997. Fracture initiation at sharp notches: Correlation using critical stress intensities. Int. J. Solid. Struct. 34, 3873-3883.

Ferro P., 2014. The local strain energy density approach applied to pre-stressed components subjected to cyclic load. Fatigue Fract. Eng. Mater. Struct. 37,1268–1280.

Gross, R., Mendelson, A., 1972. Plane Elastostatic Analysis of V-Notched Plates. Int J. Fract. Mech. 8, 267-276.

Haibach, E., 1989. Service Fatigue-Strength – Methods and data for structural analysis. Dusseldorf, VDI.

Kihara, S., Yoshii, A., 1991. A strength evaluation method of a sharply notched structure by a new parameter, “The Equivalent Stress Intensity Factor”. JSME International Journal 34, 70-75.

Jiang, Y., Feng, M., 2004. Modeling of fatigue crack propagation. Journal of Eng. Mater. Techn. 126, 77-86.

Lassen, T., 1990. The effect of the welding process on the fatigue crack growth. Welding J. 69, Research Supplement, 75S-81S.

Lazzarin, P., Tovo R., 1996. A unified approach to the evaluation of linear elastic fields in the neighbourhood of cracks and notches. Int. J. Fract. 78, 3-19.

Lazzarin, P., Tovo, R., 1998. A Notch Intensity Approach to the Stress Analysis of Welds. Fatigue Fract. Eng. Mater. Struct. 21,1089-1104.

Lazzarin, P., Zambardi, R., 2001. A finite-volume-energy based approach to predict the static and fatigue behaviour of components with sharp V-shaped notches. Int. J. Fract. 112, 275-298.

Lazzarin, P., Sonsino, C.M., Zambardi, R., 2004. A Notch Stress Intensity approach to predict the fatigue behaviour of T butt welds between tube and flange when subjected to in–phase bending and torsion loading. Fatigue Fract. Eng. Mater. Struct. 27, 127-141.

Lazzarin, P., Berto, F., Gomez, F.J., Zappalorto, M., 2008. Some advantages derived from the use of the strain energy density over a control volume in fatigue strength assessments of welded joints, Int. J. Fatigue, 30, 1345-1357.

Lazzarin, P., Berto, F., Zappalorto, M., 2010. Rapid calculations of notch stress intensity factors based on averaged strain energy density from coarse meshes: Theoretical bases and applications. Int. J. Fatigue 32, 1559–67.

Livieri, P., Lazzarin, P., 2005. Notch Stress Intensity Factors and fatigue strength of aluminium and steel welded joints. Int J. Fract 133, 247-276.

Meneghetti, G., Campagnolo, A., Berto, F., Atzori, B., 2015. Averaged strain energy density evaluated rapidly from the singular peak stresses by FEM: cracked components under mixed-mode (I+II) loading. Theor. Appl. Fract. Mech. 79, 113–124.

Yakubovskii, V.V., Valteris, I.I., 1989. Geometrical parameters of butt and fillet welds and their influence on the welded joints fatigue life. International Institute of Welding, Document XIII-1326-89.

Qian, J., Hasebe, N., 1997. Property of eigenvalues and eigenfunctions for an interface V-notch in antiplane elasticity. Eng. Fract. Mech. 56, 729–734.

Radaj, D., 1990. Design and analysis of fatigue resistant welded structures, Abington Publishing, Cambridge.

Radaj, D., 2014. State-of-the-art review on extended stress intensity factor concepts. Fatigue Fract. Eng. Mater. Struct. 37, 1–28.

Radaj, D., 2015. State-of-the-art review on the local strain energy density concept and its relation to the J-integral and peak stress method. Fatigue Fract. Eng. Mater. Struct. 38, 2–28.

Rulmeca Bulk Catalogue, 2014

Seweryn, A., Poskrobko, S., Mróz, Z., 1997. Brittle fracture in plane elements with sharp notches under mixed-mode loading, J. Eng. Mech. 123, 535-543.

Sheppard, S.D., 1991. Field effects in fatigue crack initiation: long life fatigue strength. Trans. ASME, J. Mech. Design 113, 188-194.

Singh, P.J., Achar, D.R.G., Guha, B., Nordberg H., 2003a. Fatigue life prediction of gas tungsten arc welded AISI 304L cruciform joints different LOP sizes. Int. J. Fatigue 25, 1-7.

Singh, P.J., Guha, B., Achar, D.R.G., Nordberg, H., 2003b. Fatigue life prediction improvement of AISI 304L cruciform welded joints by cryogenic treatment. Eng. Fail. Anal. 10, 1-12.

Sonsino, C.M., 1995. Multiaxial fatigue of welded joints under in-phase and out-of-phase local strains and stresses. Int J. Fatigue 17, 55-70.

Taylor, D., Barrett, N., Lucano, G., 2002. Some new recent methods for predicting fatigue in welded joints. Int J. Fatigue 24, 509-518.

Williams, M.L., 1952. Stress singularities resulting from various boundary conditions in angular corners of plates in extension. J. Appl. Mech. 19, 526-528.

Zappalorto, M., Lazzarin, P., Yates, J.R., 2008. Elastic stress distributions resulting from hyperbolic and parabolic notches in round shafts under torsion and uniform antiplane shear loadings. Int. J. Solid. Struct. 45, 4879-4901.